Curr Cardiovasc Imaging Rep (2012) 5:481–490
DOI 10.1007/s12410-012-9160-6

Multimodality Imaging in Congenital Heart Disease: an Update

Uyen T. Truong · Shelby Kutty · Craig S. Broberg · David J. Sahn

Published online: 9 August 2012

Abstract The increasing number of survivors of congenital heart disease (CHD) has been paralleled by advancement of imaging modalities used for the ongoing assessment of these patients. There has been a large body of literature describing new approaches to non-invasive assessment of CHD. We will review new applications of well established as well as novel techniques for the management and understanding of CHD.

Keywords Congenital heart disease · Multimodality imaging · Echocardiography · Magnetic resonance imaging · Computed tomography · Angiography

Introduction

The increasing number of survivors of congenital heart disease (CHD) has been paralleled by advancement of imaging modalities used for the ongoing assessment of these patients. In 2005, it was estimated that 600,000 adults have moderate to severe complex CHD and that 1,000,000 people live in the US with adult congenital heart disease (ACHD). The Center for Disease Control Multiple Cause-of-Death registry reports a significant drop in mortality for all ages, some with complex CHD, from 1979-2005 [1]. The management of these patients with complex CHD with the added complexity of post-operative surgical intervention and scarring requires multimodality imaging to comprehend their physiology and anatomy.

A large body of literature describing new approaches to non-invasive assessment of CHD has emerged. We will review new applications of established and novel techniques for CHD based on studies that have been published in the past few years. This is to update the reader on the state of knowledge in this vastly changing field. For conciseness, we will focus only on literature on human subjects and limit our discussions to original research with minimal mention of review articles. The imaging modalities discussed will be those novel to clinical as well as to the research arena. We will explore speckle tracking of the left and right ventricle (RV) for the determination of 2-dimensional (2D) and 3-dimensional (3D) strain, torsion, and volume assessment of the RV. Magnetic resonance imaging (MRI) methods reviewed will address volume imaging, evaluation for ventricular ischemia and fibrosis, MRI spatial modification of magnetization (SPAMM) tagging, and displacement encoding with stimulated echoes (DENSE) for defining cardiac deformation. Computed flow dynamics will be addressed. We will also discuss fetal imaging for prenatal diagnosis of CHD using echocardiography and MRI. Finally, we will discuss the advances in cardiac catheterization and electrophysiology with 3-dimensional rotational angiography (3DRA) and 3D electroanatomic mapping.

Echocardiography

B-mode ultrasound-based imaging, color and spectral Doppler, remain the mainstay of managing patients with CHD. 2D and recently, 3D echocardiography continue to

U. T. Truong
Children's Hospital Colorado,
University of Colorado School of Medicine,
Aurora, CO, USA

S. Kutty
Children's Hospital and Medical Center,
University of Nebraska Medical Center/Creighton University,
Omaha, NE, USA

C. S. Broberg
Oregon Health & Science University,
Portland, OR, USA

D. J. Sahn (✉)
L608, Pediatric Cardiology, Oregon Health & Science University,
3181 SW Sam Jackson Park Road,
Portland, OR 97239-3098, USA
e-mail: sahnd@ohsu.edu

be critical in answering ongoing questions about CHD. Recently, the American Society of Echocardiography Pediatric and Congenital Heart Disease Council published standard recommendations for optimization of images and measurements of cardiovascular structures in children [2•].

Jegatheeswaran et al. [3•] looked again at using the atrioventricular (AVV) valve index (left AVV area/total AVV area) in balanced and unbalanced atrioventricular septal defects in association with surgical outcomes. This study included cases from 2000-2006 seen at the four Congenital Heart Surgeons' Society member institutions. Within an index of 0.2 to 0.4, there was heterogeneity in repair approaches involving both biventricular and univentricular repairs and a higher mortality rate compared to those with an index <0.19 (univentricular repair) and >0.6 (biventricular repair). The limitation to this study is the heterogeneity of the surgeons and institutions that participated, as well as the high-risk referral nature of these centers. Nonetheless, it points out the need for clarification of defining balanced versus unbalanced atrioventricular septal defects and subsequent management strategies.

Accurate assessment of aortic regurgitation severity in pediatrics remains challenging. Beroukim et al. [4] developed a model using the parasternal vena contracta-derived area/body surface area and abdominal aorta Doppler-derived velocity time integral/antegrade velocity time integral in comparison to regurgitant fraction by MRI. Of 174 echocardiographic studies, 43 had a paired MRI performed, making the power of the study quite low. In addition, limitation of the study is that velocity time integral is angle dependant.

The role of echocardiography to delineate extracardiac vasculature is limited. Stern et al. [5] showed that in patients being evaluated for a bidirectional Glenn procedure (the second to last stage in surgical palliation for single ventricle (SV) anatomy) that echocardiography had only 59 % agreement in the presence or absence of pulmonary branch stenosis. The actual percentage, of course, depended on institution experience and protocol. However, this is an excellent example of the need for using multiple image modalities to plan surgical repair.

3-Dimensional Echocardiography

Among the most exciting development in echocardiography is real time 3-dimensional echocardiography (RT3DE). Successful 3D visualization of cardiac structures can facilitate better visualization of morphology and estimate chamber size and function [6] (Fig. 1a). Transesophageal RT3DE has been used in adults (Fig. 1b) but pediatric-sized 3D probes have not yet been developed.

Performed properly, RT3DE can demonstrate anatomy and potential etiology of AVV dysfunction. Takahashi et al. [7] described the complementary use of 2D and RT3DE technology to identify the mechanisms of AVV regurgitation

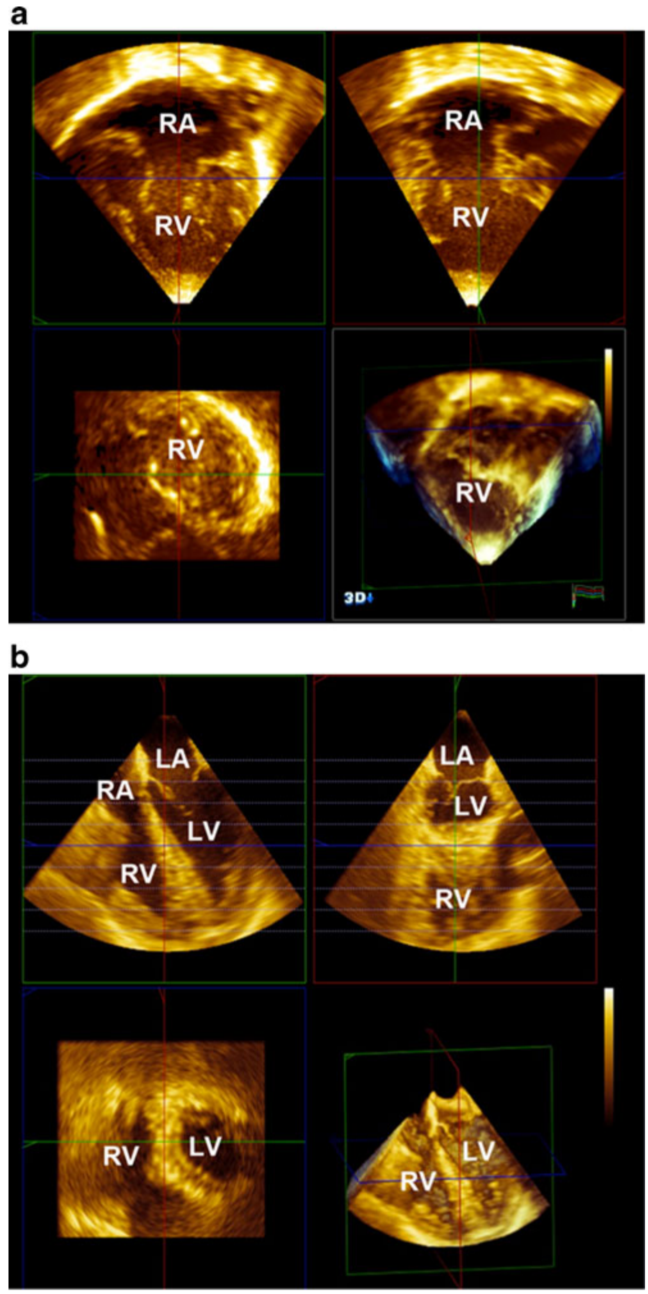

Fig. 1 3-dimensional echocardiography of a patient with hypoplastic left heart syndrome by transthoracic approach (**a**) and in a normal subject by transesophageal approach (**b**). In each box, images include the apical view (top left), 2-chamber view (top right), axial view (bottom left), and pyramidal full volume of the heart (bottom right)

in different forms of CHD, incorporating surgical findings as the reference standard. The authors showed that RT3DE was superior to 2D echocardiography in defining the regurgitant jet for both left and right atrioventricular valves, with good agreement with surgical findings. However, experience and training are required for proper interpretation and manipulation of 3D images, and remain the factors limiting more widespread use in pediatrics.

Friedberg et al. [8] used 3D echocardiography to determine left ventricular (LV) volume, mass, and ejection fraction validated against MRI in 35 children <4 years of age, four of whom had questionably small LVs. While there were correlations between the two techniques for mass, volume, and ejection fraction (EF), echocardiography derived EF showed statically significant lower EF ($p=0.0004$) and higher end-systolic volume ($p=0.0013$). Similarly, Van der Zwann et al. [9] analyzed RT3DE using the Tomtec analysis program (Tomtec Inc, Germany) in 100 patients with various CHD involving RV, LV, and biventricular pathology. This was compared to MRI obtained within 2 hours of the RT3DE. RV volume and ejection fraction showed good agreement with MRI. This finding was supported by Grewal et al. who also compared RT3DE and MRI in patients with severe pulmonary regurgitation [10]. Kutty et al. [11] showed that RT3D can be used to serially follow RV volume and ejection fraction in 18 patients with hypoplastic left heart syndrome, a group in which other modalities to correlate RT3D findings are less well established.

Doppler Tissue Imaging (DTI)

Doppler Tissue Imaging (DTI) is another non-geometric echocardiographic technique that has growing applications for assessment of global and regional myocardial function in CHD. DTI allows quantitative assessment of regional ventricular function based on myocardial velocity estimation. DTI optimizes high amplitude, low frequency signals within the myocardium after filtering out the low amplitude, high frequency signals within the blood pool. DTI-derived indices have the advantage of being relatively independent of ventricular geometry and less influenced by restricted acoustic windows. Myocardial velocities can be measured using pulsed-wave Doppler technology or the newer color-coded tissue Doppler myocardial imaging technology. DTI has been used in pediatric and adult CHD, however it does have limitations. Being a Doppler technique, DTI is angle-dependent. DTI velocities are also affected by myocardial translation and tethering.

Retrosternal areas, such as the RV, may still be difficult to visualize especially in larger individuals. These limitations apply to Doppler based color myocardial velocity encoded deformation imaging (strain and strain rate) as well.

Speckle Tracking Imaging

Speckle tracking imaging (STI) is a newer ultrasonic tool for deriving objective information about myocardial cardiomechanics. “Speckles” are natural acoustic markers in ultrasound image that are tracked from frame to frame in two dimensions. A similar tool, Velocity Vector Imaging (VVI, Siemens Medical Solutions, Palo Alto, CA), uses a “feature tracking” algorithm that combines speckle tracking, AVV annulus motion, myocardial blood interface, and myocardial structure. STI imaging algorithms follow myocardial motion and are not angle-dependant. From this, strain, the percentage of change in length compared to the original length, and strain rate, the derivative of strain over time, can be derived. These are less preload dependant than DTI, and are thought to be a better reflection of contractility [12]. Strain is influenced by weight, blood pressure, and heart rate, and has been shown in multiple studies [13–15] to detect early signs of myocardial dysfunction before changes in ejection fraction or symptoms are noted. Longitudinal (Fig. 2a), radial, and circumferential (Fig. 2b) strain can be derived. On short axis images, rotation can also be determined.

Initially used to describe regional myocardial deformation in ischemic heart disease, this technique has been widely adopted in CHD research over the past several years.

a

b

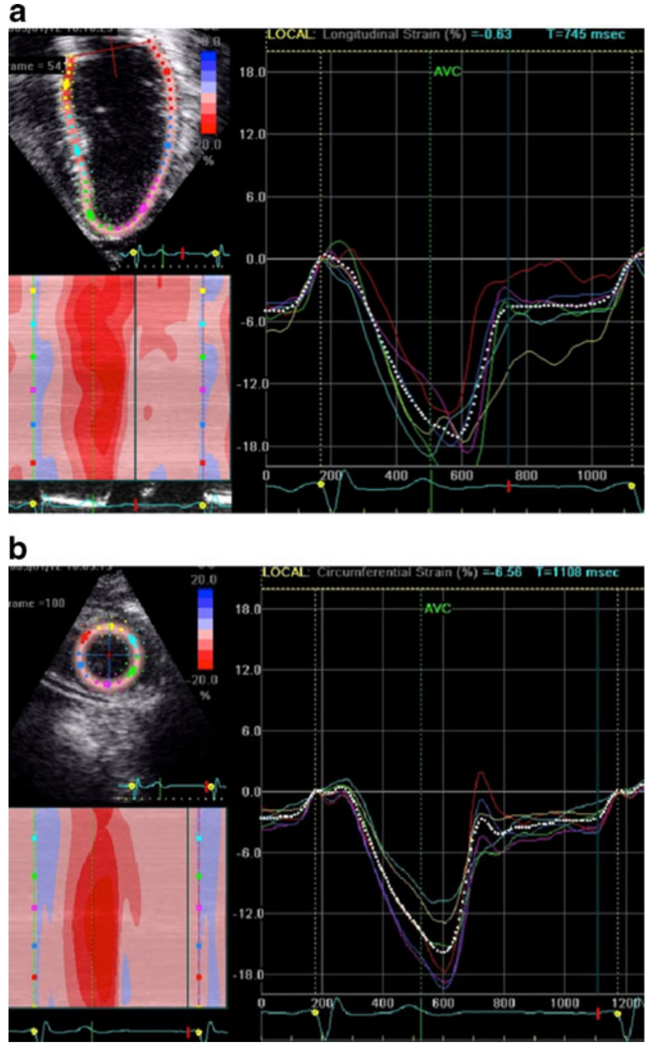

Fig. 2 Longitudinal strain obtained in the 4-chamber view of a normal patient (**a**); note uniformity of strain curves from the different segments of the myocardium. Circumferential strain curve of the left ventricle in short axis derived normal patient (**b**)

However, intraobserver and interobserver variability has been an obstacle for incorporating these values into clinical practice. Also, while some deformation parameters are similar between different software packages, others including radial strain and strain rate are significantly different. This was shown by Kopman et al. [16] who compared myocardial deformation as obtained using Vivid7 and iE33 ultrasound systems, analyzed offline by EchoPac version 7.0, QLAB version 7.0 (Philips Medical Systems), and SPEQLE. This is to be distinguished from feature tracking by VVI, which was mentioned above [17]. Low frame rates are also major limitations to STI, especially in retrospective studies.

Markus et al. [18] utilized this method to examine deformation in 37 children with valvar aortic stenosis before balloon valvuloplasty and then 6 months and 3 years following the procedure. Compared to 74 age-matched normal controls and 76 uncorrected valvar aortic stenosis, the study group had decreased longitudinal, circumferential, and radial strain at baseline compared to both control groups. Significant increase in strain was seen at 6 months follow-up ($p<0.01$), but at 3 years, all strain parameters in study group were less than normal ($p<0.05$). Singh et al. [19] studied 15 patients after the Fontan procedure compared to 22 normals using STI derived strain and tissue tagging MRI sequences (discussed below). The authors found higher correlation with global strain than they did regional strain, calling into question the contribution of some wall segments to overall function and emphasizing the effects of abnormal geometry on overall ventricular mechanics.

STI can also be used for dyssynchrony studies. Hui et al. [20] showed this using DTI and STI (EchoPac, GE) in determining RV synchrony in 103 healthy children. The difficulty of obtaining adequate RV images in addition to the retrospective nature of this study, limit the interpretation of this study.

Similar to findings in SV patients after the Fontan procedure (completion of SV palliation involving anastomosis of the inferior vena cava to the pulmonary circulation) [21], Moiduddin et al. [22, 23] found that in both left (mean age 7.1 ± 2.8 years) and right morphologic SV roughly 7 years after the Fontan procedure had regional decrease in strain and strain rate even at an early age.

Recently, 3D-STI has been applied for the estimation of LV regional strain components and has shown reasonable correlation with sonomicrometry [24]. Determination of radial strain using a 3D-STI system from a pyramidal 3D dataset has been successfully used to quantify 3D LV dyssynchrony [25]. However, early results comparing 2D and 3D-STI in the assessment of longitudinal, circumferential, and radial strain of the LV have shown discordance in the strain values obtained [26] and suboptimal correlation suggesting that the two techniques are not interchangeable [27].

Fetal Echocardiography

The ability to accurately detect and diagnose CHD in fetuses has allowed optimization of perinatal care and parental counseling, as well as improved morbidity and mortality of fetuses with CHD [28–30]. Fetal echocardiograms are being done at earlier gestational age (Fig. 3), although first trimester screening, while feasible, may miss CHD due to imaging limitations and the progressive nature of certain lesions [31]. In the more common screening period of second trimester, imaging of fetal hearts is limited by gestational age, maternal obesity and scarring, the presence of oligohydramnios, and fetal position [32, 33]. 3D fetal imaging is still in very early stages.

Left Ventricular Torsion

2D-STI derived torsional mechanics provide new insights into LV systolic and diastolic function [34, 35]. The heart maintains a constant LV torsion and rotation profile when normalized by LV length and cardiac cycle, and in children, tend to twist, untwist and deform faster than in older subjects [36]. 2D-STI derived LV twist is decreased in apical hypertrophic cardiomyopathy, which suggests that regional myocardial changes can modify the global LV twist mechanics [37].

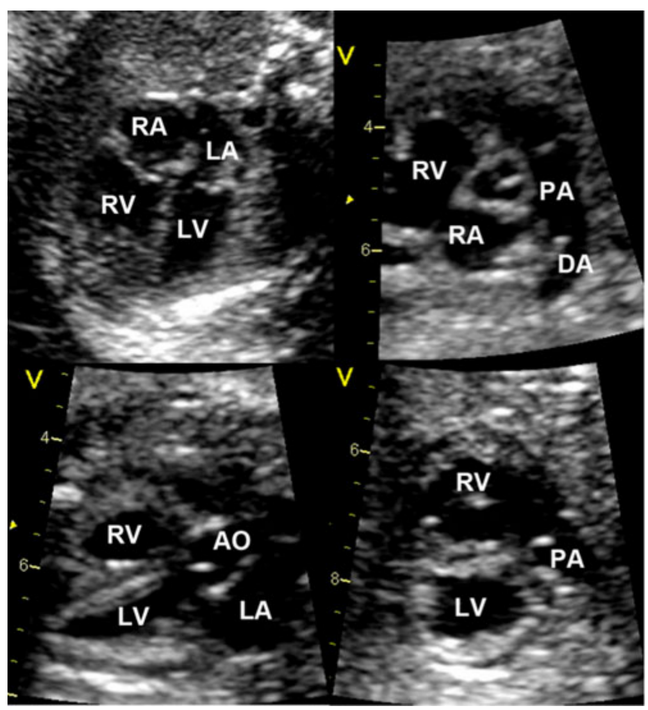

Fig. 3 Fetal echocardiogram during the second trimester can clearly show cardiac anatomy and ventricular size. This image depicts a normal 4-chamber view of the heart (top left), short axis (top right), left ventricular outflow tract (bottom left), and right ventricular outflow tract (bottom right)

Using 2D-STI, Popescu et al. have shown significant relationship between the time to peak LV untwisting rate and LV filling pressures in patients with severe aortic stenosis and preserved LV ejection fraction [38].

Cardiac Magnetic Resonance Imaging

MR is ideally suited for CHD management. It provides high-resolution, highly accurate images of cardiac and vascular anatomy, tissue characterization, detection of viable and fibrotic myocardium by delayed enhancement via 2D imaging. It now also allows tissue tagging and DENSE, flow dynamics with phase contrast (PC) utilizing 3D spatial encoding to provide 4D flow MRI.

Although quantification of ventricular volume is a crude metric of myocardial contractility, it is still indispensable, and often a challenge to obtain in CHD. MRI is well-suited for RV volume and function assessment, as is required in tetralogy of Fallot (TOF), pulmonary atresia, transposition, or Ebstein anomaly [39]. MRI has found a strong niche in this field, and is an indispensible modality for any ACHD center [40]. However, there is an ongoing controversy as to the approach, axial versus multiplanar stacks. The multiplanar approach takes longer to acquire using breath-hold sequences, but enables clearer visualization of the valve plane, and advantage in quantifying systolic RV volume. Clarke et al. compared RV volume derived from both axial and short axis planes as compared to PC-derived forward flow, in a retrospective study of patients with RV volume and pressure overloaded RV [41]. The authors found no clinically meaningful difference between the two techniques, although at RV volumes $\geq$150 ml/m2, volume determined by axial plane images correlated better with PC-determination of flow in the main pulmonary artery. However, errors can occur with PC- derived forward flow in lesions with unusual flow patterns.

Ventricular Mechanics

Tagging. Tagging was one of the first MR applications for studying myocardial mechanics [42, 43] (Fig. 4). Cine MRI images are acquired after application of a prepulse to nullify signal within defined parallel lines or grids known as "tags" which persist through the cardiac cycle. The low signal intensity lines allow tracking of the myocardium through systole and diastole. The tag lines can be placed in any orientation in any cardiac plane, meaning motion can be interpreted irrespective of the transducer position. The method has evolved substantially since early uses [44–47], including the important adaptation of SPAMM allowing overlapping lines placed in perpendicular planes creating a two dimensional grid [48]. Temporal resolution differences with echocardiography means quantified results should not be comparable.

Chen et al. [49] applied a tagging sequence to the RV in long axis in 84 patients with CHD: 56 with repaired teratology of Fallot, 28 with atrial septal defects (ASD) with and without pulmonary hypertension. Compared to normal controls, patients with TOF and ASDs with pulmonary hypertension had decreased displacement with non-significant differences in ejection fraction. The utilization of the long axis removes the RV outflow tract as confounding factors, since patients with major reconstruction of the outflow tract will affect the displacement in that region. However, tagging works well for the RV with thicker walls.

DENSE. One of the most recently developed CMR tool for ventricular mechanics is known as DENSE (Fig. 5). Like tagging, DENSE imaging quantifies rotation and strain through three dimensions, with comparable temporal resolution to echocardiography though with better spatial resolution such that displacement of small areas of tissue can be tracked accurately. Epicardial and endocardial motion can be quantified differently, a task that is less reliable with tagging. DENSE has been used to show small areas of functional recovery after a myocardial infarction [50]. Resolution is proportional to scan time, and significantly longer scan times can be a limitation.

Feature tracking. Similar to speckle tracking in echocardiography, feature tracking, wherein a unique region is identified and used to follow motion through the cardiac cycle, can

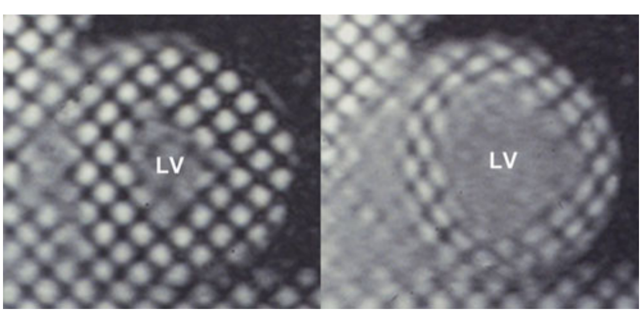

Fig. 4 MRI tissue tagging sequence in a normal patient depicting regions of myocardium in systole (left) and diastole (right)

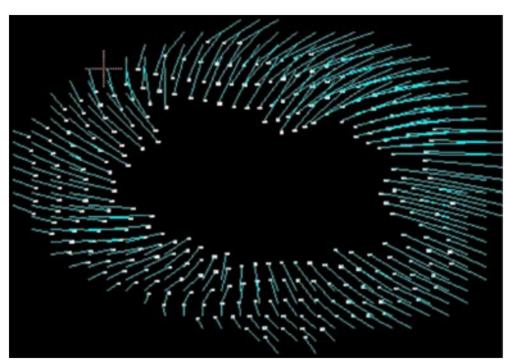

Fig. 5 DENSE imaging of the left ventricle. Note the vectors depicting outward movement during diastole

be applied to SSFP cines to track myocardial motion including strain and twist [51]. The method has the advantage of being applicable even retrospectively using standard cine images acquired during an ordinary study. We described the application of VVI for the study of SV patients [51].

Late Gadolinium Enhancement

Widely used in adults for myocardial infarction, late gadolinium enhancement (LGE) is an MRI sequence that determines the presence, extent, and pattern of cardiac fibrosis. Rathod and colleagues reported a retrospective study analyzing MR studies with LGE sequences in patients following the Fontan procedure [52]. This study included 103 studies in 90 patients (mean age 23.1±10.9 years), and showed that lower ejection fraction, higher end-diastolic volume, higher ventricular mass, and higher frequency of non-sustained ventricular tachycardia were associated with larger percentage of LGE. Twenty-eight percent had positive LGE despite the relatively young age of the cohort, albeit the cause of fibrosis was not evaluated.

While late gadolinium enhancement detects dense fibrosis or "replacement" fibrosis, many CHD patients likely have diffuse fibrosis that may defy detection with standard techniques. Newer methods utilize T1 mapping of myocardium to quantify the partition coefficient of gadolinium or the volume of distribution of gadolinium, a measure of extracellular volume. This parameter is objective, independent of gadolinium dose, and also imaging timing. We described our experience with T1 mapping in 50 patients with CHD (mean age 37± 12 years) [53], including systemic RV, repaired TOF, and cyanosis. The volume of distribution, or "fibrosis index" was higher in CHD patients than normal controls, and correlated with ventricular enlargement and worsening ventricular function. Further studies on a larger scale using the fibrosis index in association with clinical parameters offer an exciting method by which we can follow ventricular changes serially in ACHD.

4D Flow

Hemodynamics and flow dynamics can be determined by using MRI, along with high-resolution images of the heart and vasculature (Fig. 6a). This is achieved by flow-sensitive 3D MRI imaging, otherwise known as 4D flow MRI, time resolved 3D velocity mapping with three- directional velocity encoding, or 4D PC-MRI. Visualization of local and global blood flow characteristics can be achieved by this method. Barker and colleagues [54] described the use of wall shear stress by phase contrast MR imaging in CHD. Fifteen patients with bicuspid aortic valves (BAV) were shown to have increased wall shear stress in the ascending aorta is elevated in the patients when compared to normal subjects. Elevated wall shear stress can affect vascular injury and remodeling, ultimately leading to aneurysm formation [55]. Hope et al. also described 4D flow in BAV patients depicting eccentric helical flow [56]. Later, Hope and colleagues published their report on wall shear stress determination by 4D flow on 20 patients with normal aortic valves and 26 patients with BAV [57]. The BAV subgroup with eccentric flow had higher flow asymmetry than the BAV with normal flow. It is unclear from this paper the effect of repaired aortic coarctation on the wall shear stress in the three subgroups, since all three groups included these patients. Any residual aortic distortion may have flow asymmetry, which can affect upstream flow as well.

In a study of ten patients (mean age 12.1 years, ranging 2-24 years) with repaired TOF and four healthy controls (mean age 26 years, ranging 25-27 years), Geiger and colleagues compared flow velocity, retrograde flow, and pathologic vortices within ventricular chambers with 4D flow MRI [58] (Fig. 6b). The patient population was too small to draw many conclusions. However, the authors showed feasibility of 4DMRI in TOF patients, which may prove to be useful for determining risk factors for vessel dilation and aneurysm formation, and to tailor surgical approaches.

Fetal Cardiac MRI

A small number of publications have emerged examining the feasibility and utility of cardiac MRI during the fetal state (Fig. 7). Several factors limit the feasibility of cardiac MRI and affect clinical utility. Loomba and colleagues [59] noted that one of the obstacles for fetal cardiac MRI is fetal

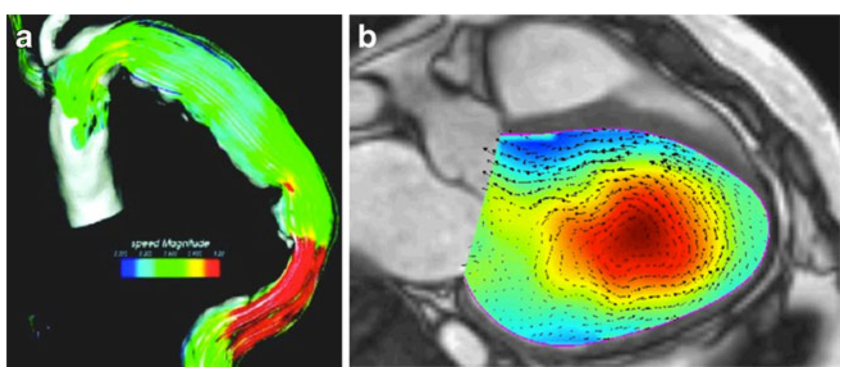

Fig. 6 4D flow imaging of a tortuous aorta (**a**) with velocity change through the region of the distorted isthmus, as shown by the color change of flow. 4D depiction of vortex with a normal left ventricle with the highest velocity seen in the center of the chamber (**b**)

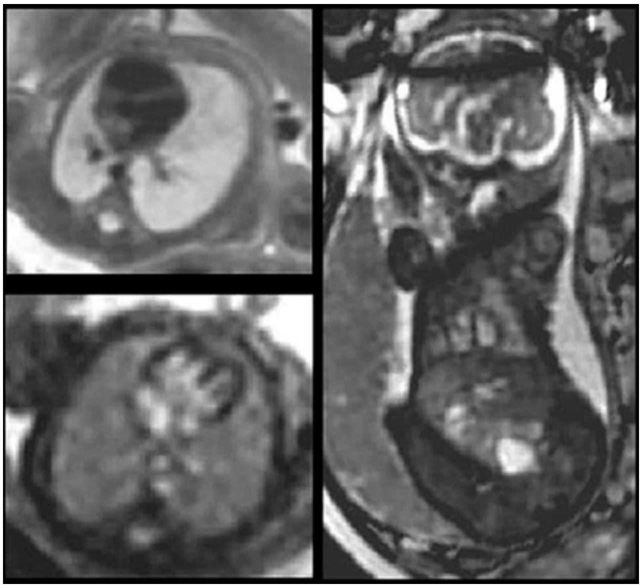

Fig. 7 Fetal cardiac MRI by black blood (top left) and fast SSFP through the axial plane (bottom left) of the heart, and the entire fetus (right). Note delineation of the ventricular chamber size in the 4-chamber view

movement. This can be addressed with maternal sedation [60, 61], although this is certainly not widely used. The difficulty in monitoring fetal rhythm and pulse restricts cardiac MRI sequences that rely on electrocardiogram- or pulse monitor-gating. Fast fetal heart rates also are limitations for scan time. Techniques to overcome fetal MRI difficulties include real-time imaging, nontriggered acquisition, self-gating, and most recently, with metric gating, performed on one fetus [62]. Votino and colleagues published a cross sectional study which included 66 fetuses with normal hearts and 40 with CHD using steady-state free precession sequences [63]. The four-chamber view was seen in 98 % of all fetuses. Limited visualization of the left and right outflow tract was achieved in 50 % and 54 % in fetuses with CHD. There is significant potential for faster sequences that can clearly show fetal cardiac structures. However, for now, the clinical use of this novel approach remains limited.

Cardiac Catheterization

The cardiac catheterization laboratory has also experienced expanded utility of 3D imaging in CHD. 3D visualization of cardiovascular structures can be achieved by computed tomography (CT)/MRA overlay, 3D echocardiography, and especially 3DRA. Originally utilized for neuroradiologic endovascular procedures [64–66], 3DRA has found an increasing role in interventional radiology, interventional cardiology, and electrophysiology [67–70]. Angiographic CT images can be derived from rotational angiography using a C-arm mounted on a flat-detector detector inside the interventional lab [71]. The images can be overlaid over 2D live images under fluoroscopy providing a roadmap for interventions. Images obtained from 3DRA can be reconstructed in the interventional suite. This allows increased diagnostic accuracy of complex vascular structures while minimizing contrast as well as radiation exposure. Glatz and colleagues [71] published a study of 41 cardiac catheterization studies in patients with CHD (mean age 5.1 years), involving RV outflow tracts, pulmonary artery branch stenosis, cavopulmonary connections, and pulmonary veins. 3DRA provided additional structural details in a variety of CHD. Seventy-one percent of the 3DRA obtained were of diagnostic quality without significant increase in contrast or radiation exposure. Berman and colleagues [72] described the utility of 37 3DRA studies in 32 SV patients with cavopulmonary connection in SV patients. In this study 89 % of the 3DRA were considered to be of diagnostic quality. Impressively, the authors report 68 % of the 3DRA provided additional anatomic details compared to the biplane angiography. Fagan et al [73] reported the first successful stent angioplasty using 3DRA (Fig. 8).

Previously obtained CT or MR angiographic images can also be co-registered with volumes obtained by 3DRA [74]. However, there is little data reported on the use of this in humans with CHD. Children's Hospital of Philadelphia did recently publish their experience with fusion of X-ray and MRI images in 23 patients, mean age 3.59 years, comprised of both single and biventricular anatomy [75]. Internal markers, including bones and airways, were used with reported reduction of radiation use.

While these imaging modalities are exciting and offer immense potential, the limitation of only a small number of pathologies involving a small number of patients should not be overlooked. Furthermore, many of the larger studies

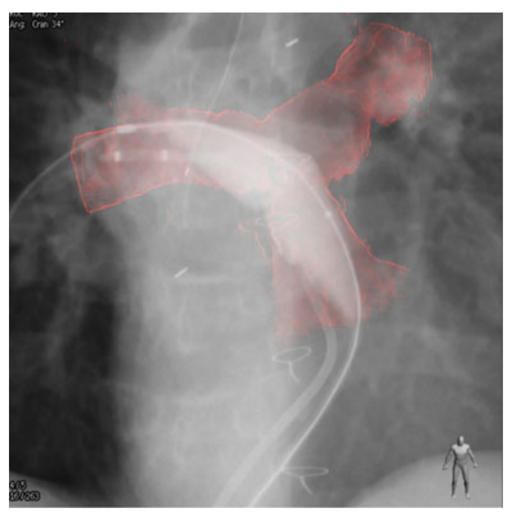

Fig. 8 Overlay of 3-dimensional rotational angiogram onto live fluoroscopic images during balloon angioplasty of the right pulmonary artery

were done retrospectively [71, 72]. Overlay with live 2D images may not align exactly due to breathing motion, patient movement, or structure displacement from interventional wires or vessel manipulation during the procedure. In these early stages, manipulation of reconstructed images to obtain appropriate spatial orientation of structures is still dependent on user and institutional experience.

RT3DE and intracardiac echocardiography (ICE) have also been used for ASD device closure [76, 77]. RT3DE can create pyramid-shaped 3D volume dataset that can be cropped in any plane. This would allow en face imaging of the ASD and the visualization of adjacent structures and defect rims. This technique in collaboration with electro-anatomic mapping programs, CartoSound (CartoSound, Biosense-Webster, Diamond Bar, CA), have also been shown to be useful for electrophysiological ablation procedures [78, 79].

Conclusions

The majority of imaging tools have only been applied to congenital heart disease in small studies in a retrospective manner. However, the potential of these methods to enhance our understanding of the clinical situations is tremendous. The CHD field must move forward toward larger multi-center research paradigms to demonstrate widespread applicability to clinical practice. An important consideration for today's imaging innovations is whether a new technique can offer substantial improvements in outcome, safety, or cost. No doubt use of complex tools to refine our diagnostic accuracy will lead us toward delivery of more sophisticated or patient-specific prevention strategies or therapies. We are excited to witness the inevitable large-scale expansion of CHD research with improved communication and collaborative work between institutions.

Acknowledgement We would like to thank the following contributors for providing us with images from their original research: Ling Li, Robin Shandas, Alex Barker, Kendall Hunter, and Thomas Fagan.

Disclosure No potential conflicts of interest relevant to this article were reported.

References

Papers of particular interest, published recently, have been highlighted as:

- Of importance

1. Pillutla P, Shetty KD, Foster E. Mortality associated with adult congenital heart disease: Trends in the US population from 1979 to 2005. Am Heart J. 2009;158(5):874–9.
2. • Lopez L, Colan SD, Frommelt PC, et al. Recommendations for quantification methods during the performance of a pediatric echocardiogram: a report from the Pediatric Measurements Writing Group of the American Society of Echocardiography Pediatric and Congenital Heart Disease Council. J Am Soc Echocardiogr: Off Publ Am Soc Echocardiogr. May 2010;23(5):465–95; quiz 576-467.*This was written by the ASE Pediatric Measurements Writing Group and includes recommended protocols for performing echocardiograms in healthy children and children with congenital heart disease.*
3. • Jegatheeswaran A, Pizarro C, Caldarone CA, et al. Echocardiographic definition and surgical decision-making in unbalanced atrioventricular septal defect: a Congenital Heart Surgeons' Society multiinstitutional study. Circulation. 2010;122(11 Suppl):S209–15. *This is complied data from 4 major surgical referall centers for congenital heart disease. Surgical results were compared with echocardiographic findings*.
4. Beroukhim RS, Graham DA, Margossian R, Brown DW, Geva T, Colan SD. An echocardiographic model predicting severity of aortic regurgitation in congenital heart disease. Circ Cardiovasc Imaging. 2010;3(5):542–9.
5. Stern KW, McElhinney DB, Gauvreau K, Geva T, Brown DW. Echocardiographic evaluation before bidirectional Glenn operation in functional single-ventricle heart disease: comparison to catheter angiography. Circ Cardiovasc Imaging. 2011;4(5):498–505.
6. Shirali GS. Three-dimensional echocardiography in congenital heart disease. Echocardiography. 2012;29(2):242–8.
7. Takahashi K, Mackie AS, Rebeyka IM, et al. Two-dimensional versus transthoracic real-time three-dimensional echocardiography in the evaluation of the mechanisms and sites of atrioventricular valve regurgitation in a congenital heart disease population. J Am Soc Echocardiogr: Off Publ Am Soc Echocardiogr. 2010;23(7):726–34.
8. Friedberg MK, Su X, Tworetzky W, Soriano BD, Powell AJ, Marx GR. Validation of 3D echocardiographic assessment of left ventricular volumes, mass, and ejection fraction in neonates and infants with congenital heart disease: a comparison study with cardiac MRI. Circ Cardiovasc Imaging. 2010;3(6):735–42.
9. van der Zwaan HB, Helbing WA, Boersma E, et al. Usefulness of real-time three-dimensional echocardiography to identify right ventricular dysfunction in patients with congenital heart disease. Am J Cardiol. 2010;106(6):843–50.
10. Grewal J, Majdalany D, Syed I, Pellikka P, Warnes CA. Three-dimensional echocardiographic assessment of right ventricular volume and function in adult patients with congenital heart disease: comparison with magnetic resonance imaging. J Am Soc Echocardiogr: Off Publ Am Soc Echocardiogr. 2010;23(2):127–33.
11. Kutty S, Graney BA, Khoo NS, et al. Serial Assessment of Right Ventricular Volume and Function in Surgically Palliated Hypoplastic Left Heart Syndrome Using Real-Time Transthoracic Three-Dimensional Echocardiography. J Am Soc Echocardiogr: Off Publ Am Soc Echocardiogr. Mar 14 2012.
12. Eyskens B, Ganame J, Claus P, Boshoff D, Gewillig M, Mertens L. Ultrasonic strain rate and strain imaging of the right ventricle in children before and after percutaneous closure of an atrial septal defect. J Am Soc Echocardiogr: Off Publ Am Soc Echocardiogr. 2006;19(8):994–1000.
13. Aurigemma GP, Silver KH, Priest MA, Gaasch WH. Geometric changes allow normal ejection fraction despite depressed myocardial shortening in hypertensive left ventricular hypertrophy. J Am Coll Cardiol. 1995;26(1):195–202.
14. El-Menyar AA, Galzerano D, Asaad N, Al-Mulla A, Arafa SE, Al Suwaidi J. Detection of myocardial dysfunction in the presence of normal ejection fraction. J Cardiovasc Med (Hagerstown). 2007;8(11):923–33.
15. Vinereanu D, Ionescu AA, Fraser AG. Assessment of left ventricular long axis contraction can detect early myocardial dysfunction in

asymptomatic patients with severe aortic regurgitation. Heart. 2001;85(1):30–6.
16. Koopman LP, Slorach C, Hui W, et al. Comparison between different speckle tracking and color tissue Doppler techniques to measure global and regional myocardial deformation in children. J Am Soc Echocardiogr: Off Publ Am Soc Echocardiogr. 2010;23(9):919–28.
17. Kim DH, Kim HK, Kim MK, et al. Velocity vector imaging in the measurement of left ventricular twist mechanics: head-to-head one way comparison between speckle tracking echocardiography and velocity vector imaging. J Am Soc Echocardiogr: Off Publ Am Soc Echocardiogr. 2009;22(12):1344–52.
18. Marcus KA, de Korte CL, Feuth T, et al. Persistent Reduction in Left Ventricular Strain Using Two-Dimensional Speckle Tracking Echocardiography after Balloon Valvuloplasty in Children with Congenital Valvular Aortic Stenosis. J Am Soc Echocardiogr: Off Publ Am Soc Echocardiogr. Feb 18 2012.
19. Singh GK, Cupps B, Pasque M, Woodard PK, Holland MR, Ludomirsky A. Accuracy and reproducibility of strain by speckle tracking in pediatric subjects with normal heart and single ventricular physiology: a two-dimensional speckle-tracking echocardiography and magnetic resonance imaging correlative study. J Am Soc Echocardiogr: Off Publ Am Soc Echocardiogr. 2010;23(11):1143–52.
20. Hui W, Slorach C, Bradley TJ, Jaeggi ET, Mertens L, Friedberg MK. Measurement of right ventricular mechanical synchrony in children using tissue Doppler velocity and two-dimensional strain imaging. J Am Soc Echocardiogr: Off Publ Am Soc Echocardiogr. 2010;23(12):1289–96.
21. Truong UT, Li X, Broberg CS, et al. Significance of mechanical alterations in single ventricle patients on twisting and circumferential strain as determined by analysis of strain from gradient cine magnetic resonance imaging sequences. Am J Cardiol. 2010;105(10):1465–9.
22. Moiduddin N, Texter KM, Zaidi AN, et al. Two-dimensional speckle strain and dyssynchrony in single left ventricles vs. normal left ventricles. Congenit Heart Dis. 2010;5(6):579–86.
23. Moiduddin N, Texter KM, Zaidi AN, et al. Two-dimensional speckle strain and dyssynchrony in single right ventricles versus normal right ventricles. J Am Soc Echocardiogr: Off Publ Am Soc Echocardiogr. 2010;23(6):673–9.
24. Seo Y, Ishizu T, Enomoto Y, et al. Validation of 3-dimensional speckle tracking imaging to quantify regional myocardial deformation. Circ Cardiovasc Imaging. 2009;2(6):451–9.
25. Tanaka H, Hara H, Saba S, Gorcsan J, 3rd. Usefulness of three-dimensional speckle tracking strain to quantify dyssynchrony and the site of latest mechanical activation. Am J Cardiol. Jan 15;105(2):235–42.
26. Saito K, Okura H, Watanabe N, et al. Comprehensive evaluation of left ventricular strain using speckle tracking echocardiography in normal adults: comparison of three-dimensional and two-dimensional approaches. J Am Soc Echocardiogr. 2009;22(9):1025–30.
27. Maffessanti F, Nesser HJ, Weinert L, et al. Quantitative evaluation of regional left ventricular function using three-dimensional speckle tracking echocardiography in patients with and without heart disease. Am J Cardiol. 2009;104(12):1755–62.
28. Tworetzky W, McElhinney DB, Reddy VM, Brook MM, Hanley FL, Silverman NH. Improved surgical outcome after fetal diagnosis of hypoplastic left heart syndrome. Circulation. 2001;103(9):1269–73.
29. Kumar RK, Newburger JW, Gauvreau K, Kamenir SA, Hornberger LK. Comparison of outcome when hypoplastic left heart syndrome and transposition of the great arteries are diagnosed prenatally versus when diagnosis of these two conditions is made only postnatally. Am J Cardiol. 1999;83(12):1649–53.
30. Franklin O, Burch M, Manning N, Sleeman K, Gould S, Archer N. Prenatal diagnosis of coarctation of the aorta improves survival and reduces morbidity. Heart. 2002;87(1):67–9.
31. Volpe P, De Robertis V, Campobasso G, Tempesta A, Volpe G, Rembouskos G. Diagnosis of congenital heart disease by early and second-trimester fetal echocardiography. J Ultrasound Med: Off J Am Inst Ultrasound Med. 2012;31(4):563–8.
32. Benacerraf BR. Examination of the second-trimester fetus with severe oligohydramnios using transvaginal scanning. Obstet Gynecol. 1990;75(3 Pt 2):491–3.
33. Hendler I, Blackwell SC, Bujold E, et al. The impact of maternal obesity on midtrimester sonographic visualization of fetal cardiac and craniospinal structures. Int J Obes Relat Metab Disord: J Int Assoc Study Obes. 2004;28(12):1607–11.
34. Park SJ, Miyazaki C, Bruce CJ, Ommen S, Miller FA, Oh JK. Left ventricular torsion by two-dimensional speckle tracking echocardiography in patients with diastolic dysfunction and normal ejection fraction. J Am Soc Echocardiogr. 2008;21(10):1129–37.
35. Saito M, Okayama H, Nishimura K, et al. Determinants of left ventricular untwisting behaviour in patients with dilated cardiomyopathy: analysis by two-dimensional speckle tracking. Heart. 2009;95(4):290–6.
36. Takahashi K, Al Naami G, Thompson R, Inage A, Mackie AS, Smallhorn JF. Normal Rotational, Torsion and Untwisting Data in Children, Adolescents and Young Adults. J Am Soc Echocardiogr. Jan 22.
37. Khachatryan V, Sirunyan AM, Tumasyan A, et al. Search for dijet resonances in 7 TeV pp collisions at CMS. Phys Rev Lett. 2010;105(21):211801.
38. Popescu BA, Calin A, Beladan CC, et al. Left ventricular torsional dynamics in aortic stenosis: relationship between left ventricular untwisting and filling pressures. A two-dimensional speckle tracking study. Eur J Echocardiogr. Jan 6.
39. Warnes CA, Williams RG, Bashore TM, et al. ACC/AHA 2008 Guidelines for the Management of Adults with Congenital Heart Disease: Executive Summary: a report of the American College of Cardiology/American Heart Association Task Force on Practice Guidelines (writing committee to develop guidelines for the management of adults with congenital heart disease). Circulation. 2008;118(23):2395–451.
40. Kilner PJ, Geva T, Kaemmerer H, Trindade PT, Schwitter J, Webb GD. Recommendations for cardiovascular magnetic resonance in adults with congenital heart disease from the respective working groups of the European Society of Cardiology. Eur Heart J. 2010;31(7):794–805.
41. Clarke CJ, Gurka MJ, Norton PT, Kramer CM, Hoyer AW. Assessment of the accuracy and reproducibility of RV volume measurements by CMR in congenital heart disease. JACC Cardiovasc Imaging. 2012;5(1):28–37.
42. Zerhouni EA, Parish DM, Rogers WJ, Yang A, Shapiro EP. Human heart: tagging with MR imaging–a method for noninvasive assessment of myocardial motion. Radiology. 1988;169(1):59–63.
43. Kerwin WS, Prince JL. Cardiac material markers from tagged MR images. Med Image Anal. 1998;2(4):339–53.
44. el SH I, Stuber M, Schar M, Osman NF. Improved myocardial tagging contrast in cine balanced SSFP images. J Magn Reson Imaging. 2006;24(5):1159–67.
45. Pai VM, Axel L. Advances in MRI tagging techniques for determining regional myocardial strain. Curr Cardiol Rep. 2006;8(1):53–8.
46. Valeti VU, Chun W, Potter DD, et al. Myocardial tagging and strain analysis at 3 Tesla: comparison with 1.5 Tesla imaging. J Magn Reson Imaging. 2006;23(4):477–80.
47. Kim YJ, Choi BW, Hur J, et al. Delayed enhancement in hypertrophic cardiomyopathy: comparison with myocardial tagging MRI. J Magn Reson Imaging. 2008;27(5):1054–60.
48. Axel L, Dougherty L. MR imaging of motion with spatial modulation of magnetization. Radiology. 1989;171(3):841–5.
49. Chen SS, Keegan J, Dowsey AW, et al. Cardiovascular magnetic resonance tagging of the right ventricular free wall for the assessment

of long axis myocardial function in congenital heart disease. J Cardiovasc Magn Reson: Off J Soc Cardiovasc Magn Reson. 2011;13:80.
50. Aletras AH, Tilak GS, Natanzon A, et al. Retrospective determination of the area at risk for reperfused acute myocardial infarction with T2-weighted cardiac magnetic resonance imaging: histopathological and displacement encoding with stimulated echoes (DENSE) functional validations. Circulation. 2006;113(15):1865–70.
51. Truong UT, Li X, Broberg CS, et al. Significance of mechanical alterations in single ventricle patients on twisting and circumferential strain as determined by analysis of strain from gradient cine magnetic resonance imaging sequences. Am J Cardiol. May 15;105 (10):1465–9.
52. Rathod RH, Prakash A, Powell AJ, Geva T. Myocardial fibrosis identified by cardiac magnetic resonance late gadolinium enhancement is associated with adverse ventricular mechanics and ventricular tachycardia late after Fontan operation. J Am Coll Cardiol. 2010;55 (16):1721–8.
53. Broberg CS, Chugh SS, Conklin C, Sahn DJ, Jerosch-Herold M. Quantification of diffuse myocardial fibrosis and its association with myocardial dysfunction in congenital heart disease. Circ Cardiovasc Imaging. 2010;3(6):727–34.
54. Barker AJ, Lanning C, Shandas R. Quantification of hemodynamic wall shear stress in patients with bicuspid aortic valve using phase-contrast MRI. Ann Biomed Eng. 2010;38(3):788–800.
55. Dolan JM, Meng H, Singh S, Paluch R, Kolega J. High fluid shear stress and spatial shear stress gradients affect endothelial proliferation, survival, and alignment. Ann Biomed Eng. 2011;39(6):1620–31.
56. Hope MD, Hope TA, Urbania TH, Higgins CB. Four-dimensional flow magnetic resonance imaging with wall shear stress analysis before and after repair of aortopulmonary fistula. Circ Cardiovasc Imaging. 2010;3(6):766–8.
57. Hope MD, Hope TA, Crook SE, et al. 4D flow CMR in assessment of valve-related ascending aortic disease. JACC Cardiovasc Imaging. 2011;4(7):781–7.
58. Geiger J, Markl M, Jung B, et al. 4D-MR flow analysis in patients after repair for tetralogy of Fallot. Eur Radiol. 2011;21(8):1651–7.
59. Loomba RS, Chandrasekar S, Shah PH, Sanan P. The developing role of fetal magnetic resonance imaging in the diagnosis of congenital cardiac anomalies: A systematic review. Ann Pediatr Cardiol. 2011;4(2):172–6.
60. Weinreb JC, Lowe T, Cohen JM, Kutler M. Human fetal anatomy: MR imaging. Radiology. 1985;157(3):715–20.
61. Van de Velde M, Van Schoubroeck D, Lewi LE, et al. Remifentanil for fetal immobilization and maternal sedation during fetoscopic surgery: a randomized, double-blind comparison with diazepam. Anesth Analg. 2005;101(1):251–8. table of contents.
62. Jansz MS, Seed M, van Amerom JF, et al. Metric optimized gating for fetal cardiac MRI. Magn Reson Med: Off J Soc Magn Reson Med / Soc Magn Reson Med. 2010;64(5):1304–14.
63. Votino C, Jani J, Damry N, et al. Magnetic resonance imaging in the normal fetal heart and in congenital heart disease. Ultrasound Obstet Gynecol: Off J Int Soc Ultrasound Obstet Gynecol. Aug 11 2011.
64. Thron A, Voigt K. Rotational cerebral angiography: procedure and value. AJNR Am J Neuroradiol. 1983;4(3):289–91.
65. Soderman M, Babic D, Homan R, Andersson T. 3D roadmap in neuroangiography: technique and clinical interest. Neuroradiology. 2005;47(10):735–40.
66. Berger MO, Anxionnat R, Kerrien E, Picard L, Soderman M. A methodology for validating a 3D imaging modality for brain AVM delineation: application to 3DRA. Comput Med Imaging Graph: Off J Comput Med Imaging Soc. 2008;32(7):544–53.
67. Noble S, Miro J, Yong G, Bonan R, Tardif JC, Ibrahim R. Rapid pacing rotational angiography with three-dimensional reconstruction: use and benefits in structural heart disease interventions. EuroIntervention: J EuroPCR Collab Work Group Interv Cardiol Eur Soc Cardiol. 2009;5(2):244–9.
68. Hansis E, Carroll JD, Schafer D, Dossel O, Grass M. High-quality 3-D coronary artery imaging on an interventional C-arm x-ray system. Med Phys. 2010;37(4):1601–9.
69. Liao R, Luc D, Sun Y, Kirchberg K. 3-D reconstruction of the coronary artery tree from multiple views of a rotational X-ray angiography. Int J Cardiovasc Imaging. 2010;26(7):733–49.
70. Garcia JA, Chen J, Hansgen A, Wink O, Movassaghi B, Messenger JC. Rotational angiography (RA) and three-dimensional imaging (3-DRA): an available clinical tool. Int J Cardiovasc Imaging. 2007;23 (1):9–13.
71. Glatz AC, Zhu X, Gillespie MJ, Hanna BD, Rome JJ. Use of angiographic CT imaging in the cardiac catheterization laboratory for congenital heart disease. JACC Cardiovasc Imaging. 2010;3 (11):1149–57.
72. Berman DP, Khan DM, Gutierrez Y, Zahn EM. The use of three-dimensional rotational angiography to assess the pulmonary circulation following cavo-pulmonary connection in patients with single ventricle. Catheter Cardiovasc Interv: Off J Soc Card Angiogr Interv. Mar 14 2012.
73. Fagan T, Kay J, Carroll J, Neubauer A. 3-D guidance of complex pulmonary artery stent placement using reconstructed rotational angiography with live overlay. Catheter Cardiovasc Interv: Off J Soc Card Angiogr Interv. 2012;79(3):414–21.
74. Levitt MR, Ghodke BV, Cooke DL, Hallam DK, Kim LJ, Sekhar LN. Endovascular procedures with CTA and MRA roadmapping. J Neuroimaging: Off J Am Soc Neuroimaging. 2011;21(3):259–62.
75. Dori Y, Sarmiento M, Glatz AC, et al. X-ray magnetic resonance fusion to internal markers and utility in congenital heart disease catheterization. Circ Cardiovasc Imaging. 2011;4(4):415–24.
76. Price MJ, Smith MR, Rubenson DS. Utility of on-line three-dimensional transesophageal echocardiography during percutaneous atrial septal defect closure. Catheter Cardiovasc Interv: Off J Soc Card Angiogr Interv. 2010;75(4):570–7.
77. Perry T, Shook DC, Nhuch F, Chou H, Shernan S, Gross WL. Repairing interatrial septal defects from the operating room to the cardiac catheterization laboratory: 2D or not 2D? Semin Cardiothorac Vasc Anesth. 2011;15(1–2):8–13.
78. Forleo GB, Pappalardo A, Avella A, Visigalli L, Dello Russo A, Tondo C. Real-time integration of intracardiac echocardiography and 3D electroanatomical mapping to guide catheter ablation of isthmus-dependent atrial flutter in a patient with complete situs inversus and interruption of the inferior vena cava with azygos continuation. J Interv Card Electrophysiol: Int J Arrhythmias Pacing. 2011;30(3):273–7.
79. Kean AC, Gelehrter SK, Shetty I, Dick 2nd M, Bradley DJ. Experience with CartoSound for arrhythmia ablation in pediatric and congenital heart disease patients. J Interv Card Electrophysiol: Int J Arrhythmias Pacing. 2010;29(2):139–45.